



Ni/Al–Mg–O solids modified with Co or Cu for the catalytic steam reforming of bio-oil

J. Remón, J.A. Medrano, F. Bimbela, L. García*, J. Arauzo

Thermochemical Processes Group (GPT), Aragon Institute for Engineering Research (I3A), Universidad de Zaragoza, Mariano Esquillor s/n, E-50018 Zaragoza, Spain

ARTICLE INFO

Article history:

Received 1 June 2012

Received in revised form

26 November 2012

Accepted 13 December 2012

Available online 21 December 2012

Keywords:

Hydrogen

Bio-oil

Steam reforming

Nickel

Copper

Cobalt

Fixed bed

Fluidized bed

ABSTRACT

An environmentally friendly method of producing a hydrogen rich gas is the catalytic steam reforming of bio-oil. This requires the development of a catalyst appropriate for the process. In the present work, five different research catalysts have been prepared and tested. A Ni/AlMg catalyst was selected as a reference. Modifications to the catalyst were studied, incorporating Co or Cu by coprecipitation or by incipient wetness impregnation. The experiments took place at 650 °C and atmospheric pressure in a fixed bed and in a fluidized bed reactor, using an aqueous fraction ($S/C = 7.6 \text{ mol H}_2\text{O/mol C}$) of pine sawdust bio-oil. A spatial time (W/m_{org}) of 4 g catalyst min/g organics and an u/u_{mf} ratio of 10 (in fluidized bed) were used. In both reactors, the coprecipitated NiCo/AlMg catalyst showed the best performance. Over a period of 2 h, 0.138 g H_2/g organics and 80% carbon conversion to gas were obtained in the fixed bed reactor.

The catalyst deactivation rate was higher when the steam reforming took place in the fixed bed reactor, although the initial H_2 and CO_2 yields were higher. In contrast, the stability of the catalysts was higher in the fluidized bed reactor. Elemental analysis, FESEM and TPO analyses of some of the catalysts revealed a relationship between their stability and the quantity and characteristics of the coke deposited on their surface.

© 2012 Elsevier B.V. All rights reserved.

1. Introduction

Biomass waste processing technologies are receiving increasing attention mainly because biomass is the only renewable source of carbon that can be converted into solid, liquid and gaseous products through different conversion processes [1]. Furthermore, biomass processing meets the difficult challenge of producing energy, chemicals and fuels through so-called ecologically friendly processes.

A hydrogen rich gas can be produced by the catalytic steam reforming of the aqueous fraction of pyrolysis liquids. This was first proposed by the National Renewable Energy Laboratory (Colorado, USA) in 1994. The strategy implies the separation of the pyrolysis liquid (bio-oil), which is first obtained after flash pyrolysis of biomass, in two phases by water addition. The non-soluble fraction, consisting of lignin-derived compounds, can be used for the production of high value added chemicals, whereas the aqueous phase [2] can be catalytically reformed to produce a gas with a high H_2 content. Depending on the reaction conditions and the catalyst used, different chemicals could be produced from this H_2 rich gas in a third generation bio-refinery [3].

The catalyst plays an important role in the catalytic steam reforming of the aqueous fraction of bio-oil. Specifically, the catalyst must enhance the reaction rate of the reforming process, which includes both the reforming reaction and the subsequent water gas shift (WGS) reaction. In addition, it must have high deactivation resistance and sufficient strength if the process is to take place in a fluidized bed reactor [2,4]. A good approach to this challenge is using Ni-based catalysts. Although cost-effective and having high activity and selectivity, these catalysts are susceptible to deactivation by carbon formation on their surface [5]. There are two methods of improving their resistance to coke deactivation: the enhancement of water adsorption on the catalyst support in order to gasify the coke or its precursors by modifying the support, and the modification of the active metal surface via the presence of other metals [5,6].

In previous works with coprecipitated Ni/Al catalysts, the Ni content was optimized (28%) for the steam reforming of model compounds (acetic acid, acetol and butanol) of bio-oil [7,8]. In a further attempt to improve the catalyst, it was found that the catalyst with a relative Mg/Al molar ratio of 0.26 showed the best performance in the steam reforming of acetic acid and acetol [9] as well as in the reforming of an aqueous fraction of bio-oil [2].

The main goal of this work is to study the active phase modification of the Ni/AlMg catalyst (selected as the reference catalyst

* Corresponding author. Tel.: +34 976762194.

E-mail address: luciag@unizar.es (L. García).

in the present work) with other metals in order to improve its behaviour as well as to reach a better understanding of the main factors affecting catalyst deactivation in this process.

The modification of the nickel phases (but not the support) in order to minimize carbon formation can be performed with metals such as Co, Cu, Cr, Mo, W, Re, Sr and Sn [6]. The major carbon-preventing effect of these promoters is to block the step sites on Ni particles, preventing the creation of nucleation sites responsible for graphite formation.

The addition of tiny amounts of Co to the catalyst has been studied by different authors [5,6] who reported that Co formed alloys with Ni and possibly reduced the crystallite size. Hu et al. [10] worked with a non-supported Ni–Co catalyst with different Ni/Co ratios. They also reported that Co was more active than Ni in the water gas shift (WGS) reaction. Ramos et al. [11] investigated the steam reforming of acetol over a coprecipitated Ni–Co/Al catalyst. Bona et al. [12] studied the steam reforming of toluene using coprecipitated Ni/Al catalysts modified with cobalt, obtaining the best results when using a Co/Ni ratio of 0.10.

The literature concerning the use of Cu as a modifier in Ni/Al catalysts focuses on the thermal decomposition of methane for the production of H₂ and of both carbon nanofibers and nanotubes. In these works, the role of Cu was associated with the inhibition of the formation of encapsulating coke [13], graphite layers [14] and carbon gasification [15]. A coprecipitated NiAlCu catalyst, prepared at constant pH, was tested in the steam reforming of model compounds of biomass pyrolysis liquids (acetic acid, acetol and butanol) by Bimbela et al. [16]. The results showed that the performance of the catalyst was improved with the presence of Cu in the steam reforming of acetic acid.

Taking these factors into account, Co and Cu were selected as modifiers of the coprecipitated Ni/AlMg reference catalyst in this work. The incorporation of the modifier was carried out using two different methods: coprecipitation and incipient wetness impregnation.

The use of these tri-metallic catalysts for catalytic steam reforming or for any other application has not been reported in the literature. Therefore, this work represents a novel investigation in the search for an appropriate catalyst for the steam reforming of the aqueous fraction of bio-oil. Furthermore, the catalytic steam reforming experiments were carried out in a fixed bed and in a fluidized bed reactor in order to study how the gas–solid contact influences the reforming process in general and the catalyst performance in particular.

2. Experimental

2.1. Experimental system

The fixed bed system, shown in Fig. 1, was based on a micro-reactor test facility consisting of a fixed bed of 25 mm in height placed inside a tubular quartz reactor of 9 mm inner diameter. N₂ was used as a carrier gas to facilitate the feeding of the aqueous fraction, preventing its polymerization inside the feeding system which could plug the feed line. It was necessary to ensure that the aqueous fraction entered the reactor in liquid phase. The gaseous mixture emerging from the bed passed to a condensation system consisting of a steel vessel cooled by means of a Peltier thermoelectric cell. The non-condensable gases were analyzed online with an Agilent M3000 micro gas chromatograph equipped with thermal conductivity detectors. A more detailed description of the installation can be found in our previous communication [7].

The fluidized bed installation, shown in Fig. 2, consisted of a bench-scale installation with a tubular 2.54 cm inner diameter quartz fluidized bed reactor. The aqueous fraction was fed into the

Table 1

Characteristics of the pyrolysis liquid and its aqueous fraction.

| | Pyrolysis liquid | Aqueous fraction |
|------------------------------------|--------------------------------------|--------------------------------------|
| Elemental analysis (wt%) | | |
| C | 36.07 | 7.35 |
| H | 8.45 | 10.82 |
| N | 0.10 | 0.00 |
| O ^a | 55.37 | 81.83 |
| Water content ^b (wt%) | 36.30 | 84.23 |
| Water/carbon ratio (mol/mol) | 0.67 | 7.60 |
| Empirical formula for the organics | CH _{1.47} O _{0.48} | CH _{2.39} O _{0.71} |

^a By difference.

^b Karl–Fischer analysis, using a high level water quantification apparatus.

reactor by being sprayed through a quartz coaxial injection nozzle placed inside a cooling jacket, described elsewhere [2], to avoid the polymerization of non-volatile compounds in the injection system when introducing the feed. The gases emerging from the upper part of the reactor passed through a condensation ice trap. The non-condensable gases continued and passed through a cotton filter. Finally, the gaseous mixture leaving the filter passed to an Agilent P200 Micro gas chromatograph equipped with thermal conductivity detectors. N₂ was used as a carrier gas, as a standard gas as well as for fluidization purposes [4].

The catalytic beds consisted of a mixture of catalyst and sand, both with a particle size of 160–320 μm. A bed height of 2.5 mm and 7 cm (in fixed bed conditions) was used in the fixed bed and fluidized bed reactors, respectively. In both installations, H₂, CO, CO₂, CH₄, N₂, C₂H₄, C₂H₆ and C₂H₂ were measured online during each experiment.

All the catalytic reforming experiments were carried out at atmospheric pressure and at a temperature of 650 °C for 2 h, using a W/m_{org} (mass of catalyst/organics mass flow) of 4 g catalyst min/g organics. This corresponds to a $G_{C_1}HSV$ (volume of C₁-equivalent species in the feed at standard temperature and pressure per unit volume of catalyst, including the void fraction per hour) of about 13,000 h^{−1} [17]. For this purpose, 0.07 g and 0.5 g of catalyst were placed in the catalytic bed and a liquid flow of 0.12 mL/min and 0.76 mL/min was used in the fixed bed and in the fluidized bed reactor, respectively.

Previous to the catalytic reaction, all the catalysts were in situ reduced using a mixture of H₂ and N₂ (1:10, v/v) at 650 °C for 1 h. A u/u_{mf} ratio of 10, defined as the ratio between the superficial gas velocity and the velocity for minimum fluidization theoretically calculated [18], was used in the fluidized bed experiments.

2.2. Aqueous fraction of pyrolysis liquids

The pyrolysis liquid (bio-oil), obtained from pine sawdust and produced using a rotating cone reactor, was supplied by BTG. Its corresponding aqueous fraction was obtained by adding the pyrolysis liquid to water at a 1:2 weight ratio using a similar method to that described by Sipilä et al. [19].

The characteristics of both the raw pyrolysis liquid as supplied and its corresponding aqueous fraction as prepared are listed in Table 1.

2.3. Catalyst preparation method

Five different research catalysts were prepared in the laboratory using both coprecipitation and impregnation methods. Ni, Al and Mg were present in all the catalysts, whereas Co or Cu was added to some of them as active phase modifiers. A similar method as that described by Al-Ubaid and Wolf [20] was used for preparing the coprecipitated catalysts and supports.

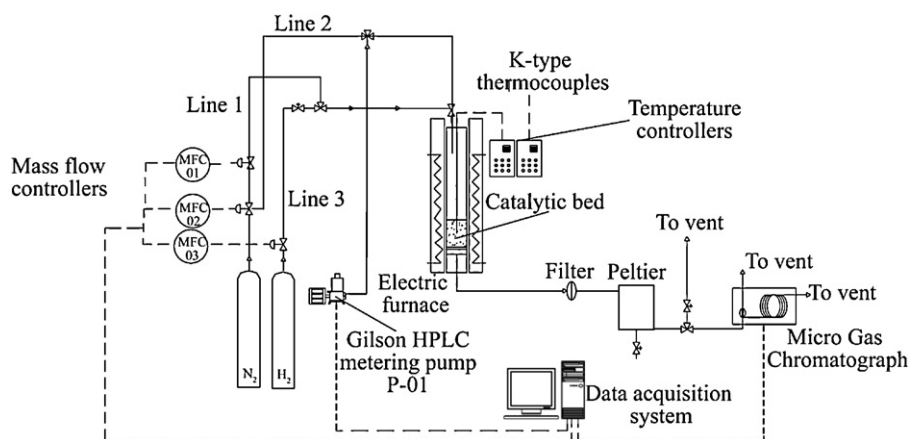


Fig. 1. Schematic of the fixed bed steam reforming experimental system.

2.3.1. Coprecipitated catalysts

Ni/AlMg, NiCu/AlMg and NiCo/AlMg catalysts were prepared using the coprecipitation method.

The coprecipitated Ni/AlMg catalyst having 28% (relative atomic percentage) Ni expressed as Ni/(Ni + Al + Mg) and a Mg/Al atomic ratio of 0.26 was selected as the reference catalyst due to its good performance when reforming model compounds of pyrolysis liquids such as acetic acid and acetol, as well as the aqueous fraction of pyrolysis liquids [2,9]. It was prepared by adding a solution of NH_4OH to a solution containing $\text{Ni}(\text{NO}_3)_2 \cdot 6\text{H}_2\text{O}$, $\text{Al}(\text{NO}_3)_3 \cdot 9\text{H}_2\text{O}$ and $\text{Mg}(\text{NO}_3)_2 \cdot 6\text{H}_2\text{O}$ dissolved in milli-Q water until a pH of 8.2 was reached. The precipitation medium was maintained at 40 °C and moderately stirred.

Both coprecipitated catalysts modified with Cu or Co (NiCu/AlMg and NiCo/AlMg) had the same nickel content as the reference catalyst, 28 at%, expressed as Ni/(Ni + Al + Mg + Cu) and Ni/(Ni + Al + Mg + Co). Cu/Ni and Co/Ni atomic ratios of 0.033 and

0.10 [12] were used when preparing the coprecipitated NiCu/AlMg and NiCo/AlMg catalysts, respectively. The preparation method of these two catalysts was similar to that already described for the reference catalyst, except for the presence of $\text{Cu}(\text{NO}_3)_2 \cdot 3\text{H}_2\text{O}$ and $\text{Co}(\text{NO}_3)_2 \cdot 6\text{H}_2\text{O}$ in the salt solution for the preparation of the NiCu/AlMg and NiCo/AlMg, respectively. The final pH was 7.9 and 8.2, respectively.

The hydrated precursors of the three coprecipitated catalysts were filtered, washed at 40 °C and dried overnight at 105 °C. Afterwards they were ground and sieved to a particle size ranging from 160 to 320 μm and calcined in an air atmosphere up to a temperature of 750 °C for 3 h.

2.3.2. Impregnated catalysts

Two impregnated catalysts (Imprg. Cu and Imprg. Co) were prepared using the reference Ni/AlMg catalyst as support, incorporating Cu or Co by incipient wetness impregnation. Solutions of

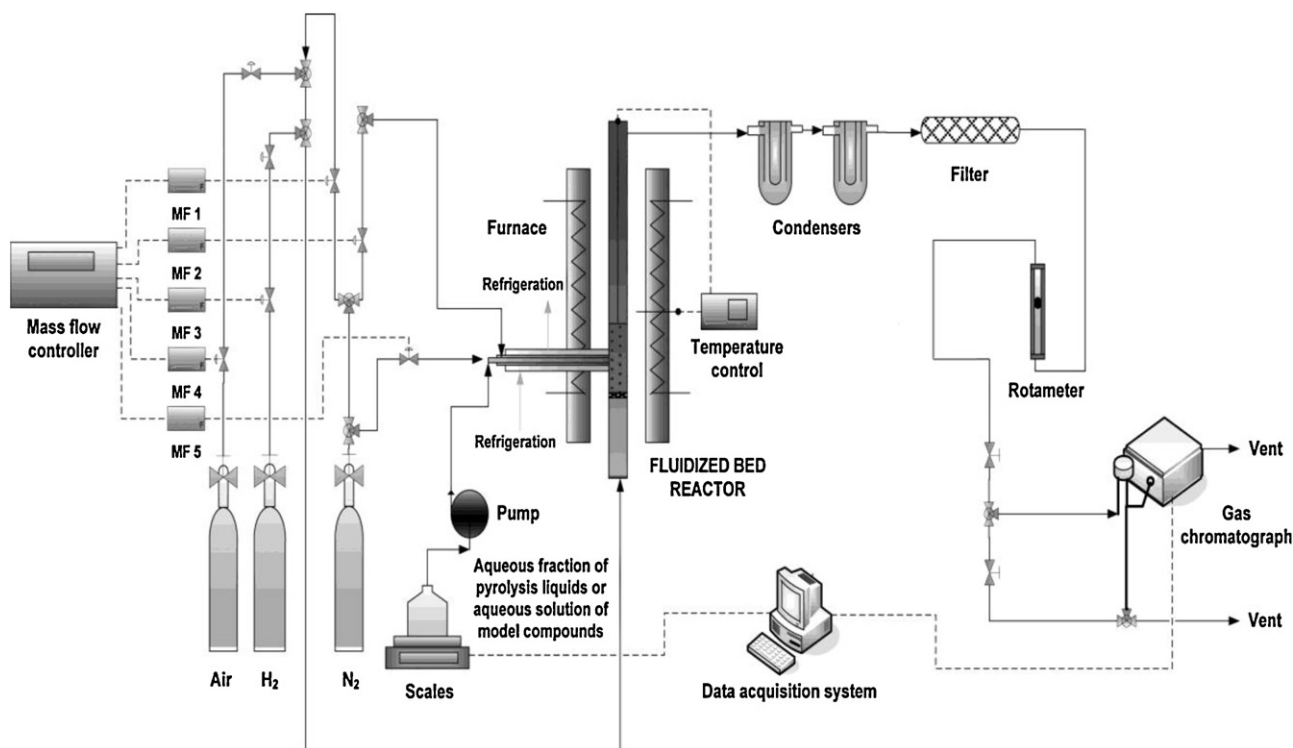


Fig. 2. Schematic of the fluidized bed steam reforming experimental system.

Table 2

Comparison between theoretical and experimental (ICP-OES) Ni/Al, Mg/Al, Cu/Ni and Co/Ni ratios.

| | Theoretical ratios (at.) | | | Experimental ratios (at.) | | |
|-----------|--------------------------|-------|----------------|---------------------------|-------|----------------|
| | Ni/Al | Mg/Al | Cu/Ni or Co/Ni | Ni/Al | Mg/Al | Cu/Ni or Co/Ni |
| Ni/AlMg | 0.49 | 0.26 | – | 0.48 | 0.23 | – |
| NiCu/AlMg | 0.49 | 0.26 | 0.033 | 0.50 | 0.24 | 0.023 |
| NiCo/AlMg | 0.49 | 0.26 | 0.10 | 0.51 | 0.23 | 0.10 |
| Imprg. Cu | 0.49 | 0.26 | 0.024 | 0.48 | 0.23 | 0.024 |
| Imprg. Co | 0.49 | 0.26 | 0.040 | 0.44 | 0.24 | 0.041 |

$\text{Cu}(\text{NO}_3)_2 \cdot 3\text{H}_2\text{O}$ and $\text{Co}(\text{NO}_3)_2 \cdot 6\text{H}_2\text{O}$ were respectively used for the preparation of the Imprg. Cu and Imprg. Co catalysts, with Cu/Ni and Co/Ni atomic ratios of 0.024 and 0.04. These ratios were lower than the respective coprecipitated ratios in order to have comparable superficial quantities of Cu and Co between the coprecipitated and impregnated catalysts. After the impregnation, the hydrated catalyst precursors were subjected to the same drying and calcination treatments as the coprecipitated catalysts.

2.4. Catalyst characterization

The fresh calcined catalysts were characterized by different techniques. These included optical emission spectrometry by inductively coupled plasma (ICP-OES), X-ray diffraction (XRD), BET nitrogen adsorption and temperature-programmed reduction (TPR).

The elemental analysis of the catalysts was carried out by ICP-OES using a Thermo Elemental IRIS INTREPID RADIAL system equipped with a Timberline IIS automatic apparatus. The samples were first dissolved (the hydrated precursors in the case of the coprecipitated catalysts and the calcined catalysts in the case of the impregnated ones) in aqua regia and diluted to a concentration approximately between 5 and 50 ppm (detection range of the instrument).

XRD patterns of the calcined catalysts were obtained with a D-Max Rigaku diffractometer equipped with a $\text{CuK}\alpha 1.2$ at a tube voltage of 40 kV and current of 80 mA. The measurements were carried out using continuous-scan mode with steps of $0.03^\circ/\text{s}$ at Bragg's angles (2θ) ranging from 5° to 85° . The phases present in the samples were defined by means of the JCPDS-International Centre for Diffraction Data 2000 database.

The textural properties of the calcined catalysts such as BET surface area and the average pore size and volume (BJH method) were calculated from N_2 physisorption isotherms, using the BET volumetric method. The N_2 adsorption-desorption isotherms were obtained at 77 K and room temperature, respectively, over the whole range of relative pressures using a TRISTAR II 300 V.608A analyser obtained from MICROMETRICS ASAP2020. The samples were previously degasified at 200°C during 8 h in N_2 flow.

The reducibility of the catalysts was analyzed by TPR. The measurements were carried out with a 10% H_2/Ar gas flow of 50 cm^3 (STP)/min from room temperature up to 1000°C at a rate of $10^\circ\text{C}/\text{min}$. The H_2 consumption was measured with a thermal conductivity detector.

Carbon deposited on some of the catalysts was characterized by field emission scanning electron microscopy (FESEM), elemental and temperature programmed oxidation (TPO) analysis. FESEM images from some of the used samples were taken with a Carl Zeiss MERLINTM microscope using an augmentation of 10,000 times. Before the analysis, the samples were covered with Pt. TPO analyses were carried out in a 20% O_2/He gas flow of 100 (STP) cm^3/min from room temperature to 900°C at a rate of $10^\circ\text{C}/\text{min}$. CO_2 generation was measured with a mass spectrometer.

3. Results and discussion

3.1. Catalyst characterization results

The results obtained in the ICP-OES analyses are summarized in Table 2, where the Ni/Al, Mg/Al, Cu/Ni and Co/Ni theoretical ratios are compared with their corresponding experimental ratios. A good concordance between theoretical and experimental values was achieved, showing adequate preparation methodologies for the incorporation of all the elements present in the catalysts. As an exception, it can be pointed out that there is a slight disagreement between theoretical and experimental Cu/Ni ratios for the NiCu/AlMg catalyst. In this case the experimental Cu/Ni ratio is slightly lower than the theoretical one, which indicates that Cu was not completely incorporated in the catalyst. This could be a result of all the ammonia complexes that can be formed during its preparation competing with the precipitation reaction, diminishing the amount of Cu precipitated. During the preparation of this catalyst, pH was fixed at 7.9. The experimental Cu content for this catalyst was 0.75 wt%, slightly lower than the theoretical value (1 wt%).

Fig. 3 shows the XRD patterns of the five fresh calcined catalysts. All the samples analyzed have wide and asymmetric peaks, which indicates quite low crystallinity, except for the NiCo/AlMg catalyst whose crystallinity seems to be slightly higher than that of the other catalysts. In addition, a NiO phase is detected in all the catalysts since they all presented a peak at 2θ angles of 75° and 79° , which is consistent with the standard pattern for this crystal phase. A NiAl_2O_4 phase might also be present in the catalysts, but due to the overlapping of NiAl_2O_4 patterns with others, its presence cannot be confirmed by the results of this technique alone.

In the reference catalyst (Ni/AlMg), Ni and Mg are present in the form of oxides (NiO, MgO) and their respective spinels (NiAl_2O_4 and MgAl_2O_4). Nevertheless, the patterns of Ni and Mg oxides have very similar diffraction angles and intensities, which makes it difficult to confirm the presence of MgO phase in the catalyst. Patterns of Ni and Mg spinels also overlap.

Analysing the other four catalyst patterns, no great differences are detected in terms of crystallinity and crystal phases, even though two different preparation methods (coprecipitation and impregnation) were used. The main difference between both Cu and Co coprecipitated and impregnated catalysts is found in the second highest intensity peak ($2\theta = 42^\circ$). This peak is slightly higher and narrower for the coprecipitated catalysts, which indicates higher crystallinity. This effect is less marked in the cobalt-modified catalysts where both peaks have similar thicknesses, although the intensity of the cobalt coprecipitated catalyst peak is slightly higher than that of the impregnated one. The peak at $2\theta = 45^\circ$ is less intense for the coprecipitated catalysts than the impregnated ones. This could indicate a higher proportion of spinel phases and a lower proportion of oxide phases in the impregnated catalysts and vice versa in the coprecipitated ones. This is consistent with the fact that an increase in the calcination time enhances the formation of spinel phases, and these two impregnated catalysts were calcined

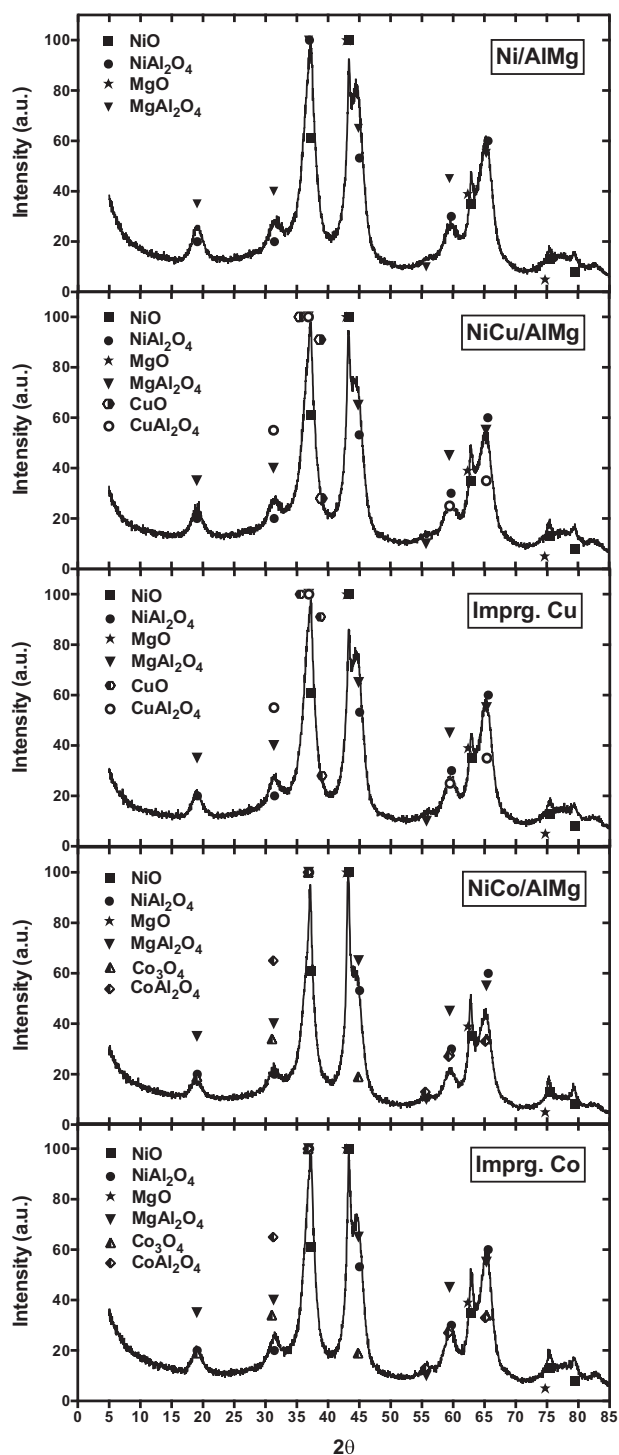


Fig. 3. XRD patterns of fresh calcined Ni/AlMg, NiCu/AlMg, Imprg. Cu, NiCo/AlMg and Imprg. Co catalysts.

twice [13,21]. Finally, the presence of Cu and Co oxides and spinel phase cannot be detected by XRD analysis alone.

The textural properties of the catalysts prepared are summarized in Table 3. All the catalysts have quite a high BET surface area. Comparing the coprecipitated with the impregnated catalysts, a slight decrease in the BET area can be seen accompanied by an increase in diameter when the modifier is incorporated into the catalysts by incipient wetness impregnation. This could be a consequence of the fact that in the impregnation preparation method, the modifiers (cobalt or copper) are present only on the catalyst surface

Table 3

Textural properties of the catalysts. S_{BET} (m^2/g), V_{pore} (cm^3/g) and D_{pore} (nm).

| | S_{BET} (m^2/g) | V_{pore} (cm^3/g) | D_{pore} (nm) |
|-----------|--|--|------------------------|
| Ni/AlMg | 137 | 0.15 | 3.7 |
| NiCu/AlMg | 126 | 0.14 | 4.8 |
| NiCo/AlMg | 132 | 0.21 | 5.1 |
| Imprg. Cu | 117 | 0.34 | 6.6 |
| Imprg. Co | 112 | 0.20 | 6.1 |

while in the coprecipitation method all the metals are coprecipitated together, leading to the modifier being incorporated not only onto the surface but also into the catalyst bulk.

From the TPR results shown in Fig. 4, two peaks (321 and 733 °C) can be appreciated in the reference (Ni/AlMg) catalyst. The first less intense peak is associated with the reduction of the NiO phase with a weak interaction with the support, which is easy to reduce. The second peak indicates the presence of the spinel (NiAl_2O_4) phase, harder to reduce due to its strong interaction with the support [2,9,22].

Two peaks are also detected in the copper-modified coprecipitated catalyst (NiCu/AlMg). The first (321 °C) might correspond to both the reduction of the bulk CuO phase, whose reduction temperature is 360 °C [23], as well as the reduction of the NiO phase. From a quantitative calculation, it was found that this peak corresponds to the reduction of 100% of the Cu and around 6% of the Ni contents of the sample. This could indicate the presence of a Cu-rich phase. This phase was not detected for the catalyst containing 1% of Cu in the work of Bimbela et al. [16], possibly due to the different preparation method used in that work. The second peak indicates the presence of the nickel spinel (NiAl_2O_4). H_2 consumption is lower when compared to the reference (Ni/AlMg) catalyst. This might indicate a lower proportion of spinel phases and consequently a higher amount of oxide phases, which is consistent with the XRD analysis as mentioned above. Two peaks are also observed in the modified copper-impregnated catalyst (Imprg. Cu). The first peak (208 °C) is very low and appears at lower temperatures than the first peak in the reference catalyst. This peak corresponds to the highly dispersed CuO contained in the catalyst [23]. From a quantitative calculation it was found that that this peak represents the reduction of 100% of the total amount of Cu present in the sample. The second peak (752 °C) appears at higher temperatures than the

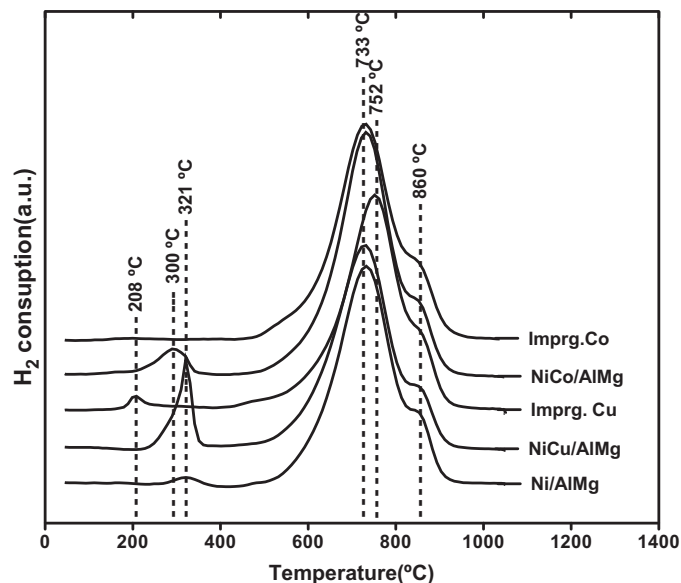


Fig. 4. TPR profiles of the Ni/AlMg, NiCu/AlMg, Imprg. Cu, NiCo/AlMg and Imprg. Co catalysts.

second peak of the reference catalyst. This could be indicative of a higher presence of spinel phases and consequently lower oxide phases in this impregnated catalyst in comparison with the reference Ni/AlMg catalyst. This is a consequence of the fact that this catalyst has been calcined twice. An increment in the calcination time leads to a higher content of spinel as well as a lower content of oxide phases [13,21].

In the cobalt-modified coprecipitated catalyst (NiCo/AlMg) two peaks are detected. The first peak appears at a temperature of about 300 °C and might correspond to the reduction of the NiO phase. The intensity of this peak is higher in the NiCo/AlMg catalyst than in the Ni/AlMg, which might indicate that this peak could be the result of both the reduction of the NiO phase as well as the reduction of the Co₃O₄ phase, which has minimal interaction with the support [24–26]. All these facts may suggest a high Ni–Co interaction [27]. The second peak (732 °C), which has the highest intensity, corresponds to the reduction of the nickel spinel (NiAl₂O₄) phase. In addition, the H₂ consumption of this second peak is higher than that of the reference Ni/AlMg catalyst, which might indicate that this peak is also a result of the reduction of cobalt species strongly interacted with the support [24–26]. In the cobalt-modified impregnated catalyst, only one peak is found in the TPR results. The lower temperature peak disappears. This disappearance might indicate that the nickel is present in the form of nickel spinel (NiAl₂O₄) and that the cobalt strongly interacts with the support [24–26].

Finally, a shoulder is detected at higher temperatures (860 °C) for all the catalysts. This shoulder probably indicates the presence of magnesium phases [2], corresponding to NiAl₂O₄ spinel units incorporated into the MgAl₂O₄ spinel structure.

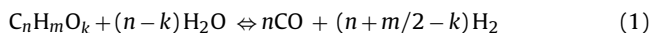
The TPR results indicate that while the two catalysts prepared by impregnation could not have low temperature reducible species of Ni ($T < 400$ °C), the catalysts prepared by coprecipitation could have.

3.2. Experimental data processing

The performance of the five prepared catalysts has been tested in the steam reforming of an aqueous fraction of biomass pyrolysis liquid in two different installations, a fixed bed reactor facility and a fluidized bed. The steam reforming reactions of any oxygenated organic compounds were first proposed by [17] and are shown as follows:

1- Reforming reactions:

Steam reforming of the oxygenated compounds

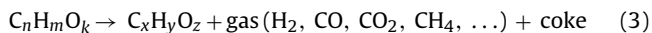


Water gas shift (WGS) reaction:



2- Other side reactions:

Thermal decomposition:



Methane steam reforming:



Boudouard reaction:



Carbon deposits gasification:



The steam reforming results for all the catalysts tested are presented in the tables and figures. The tables show the overall 2 h

values of the response variables studied (overall carbon conversion to gases, and overall H₂, CO₂, CO and CH₄ yields expressed as g of gas/g of organics fed). The evolution with time of these response variables is presented graphically.

One-way analysis of variance (one-way ANOVA) was used to evaluate the influence of the catalyst on the catalytic steam reforming. Overall carbon conversion to gas and overall H₂, CO₂, CO and CH₄ yields were compared for each catalyst to evaluate the extent of the reforming and water gas shift reactions as well as to study the catalyst deactivation. If the *p*-value obtained is lower than the significance level used ($\alpha = 0.05$), it can be concluded with 95% confidence that at least one of the catalysts provides a value of the response variable different from the others.

When the ANOVA analysis detected significant differences, the multiple range least significant difference (LSD) test with a significance level of 0.05 was employed to determine differences between pairs of catalysts. The results of this test are presented in the multiple range tables, where the catalysts are classified in homogeneous groups using as many letters as homogeneous groups obtained in the analysis. Catalysts sharing the same letter belong to the same homogenous group.

The theoretical equilibrium values were calculated using Aspen-tech HYSYS 3.2 simulation software employing a Gibbs reactor module with the PRSV thermodynamic package. This Gibbs reactor utility provides the theoretical equilibrium composition minimizing the Gibbs free energy of the system, which allows calculating the thermodynamic equilibrium without introducing the reaction stoichiometry. Acetic acid, acetol and butanol were input in the Gibbs module to model the composition of the aqueous fraction.

3.3. Results in the fixed bed reactor

Co and Cu were incorporated in the catalyst as modifiers of the active phase with the main purpose of decreasing the catalyst deactivation by coking.

The overall 2 h results obtained in the steam reforming experiments in fixed bed using the Ni/AlMg, NiCo/AlMg, NiCu/AlMg, Imprg. Co and Imprg. Cu catalysts as well as the corresponding thermodynamic equilibrium values under the operating conditions are summarized in Table 4. The statistical analysis of the results by means of an ANOVA analysis is presented in Table 5, where the *p*-values and the LSD homogeneous groups of catalysts for each response variable are given.

The overall carbon conversion to gases and the overall H₂ and CO₂ yields as well as their evolution over time give an idea of the performance of the different catalysts in terms of overall activity, initial activity and deactivation with time (Fig. 5). H₂ and CO₂ are the principal products of the reforming reaction. The ANOVA analysis of the results, shown in Table 5, shows that at least one of the tested catalysts provided different results in terms of different carbon conversion to gases and H₂ and CO₂ yields (*p*-values lower than the significance level $\alpha = 0.05$). The multiple range LSD test shows the existence of three different homogeneous groups. The best performance during the reforming of the aqueous fraction in terms of higher overall carbon conversion to gases ($80.0 \pm 4.5\%$) and H₂ (0.138 ± 0.006 g H₂/g organics) and CO₂ (1.014 ± 0.066 g CO₂/g organics) yields, which implies the highest catalyst stability, was achieved with the coprecipitated NiCo/AlMg catalyst.

Analysing the multiple range LSD test results represented in Table 5, it can be seen that both the catalyst preparation method (coprecipitation or impregnation) and the type of modifier (Co and Cu) might have a significant influence on the catalyst performance. All the coprecipitated catalysts provided statistically higher carbon conversion to gases and H₂ and CO₂ yields than the impregnated catalysts. This difference is a direct consequence of the

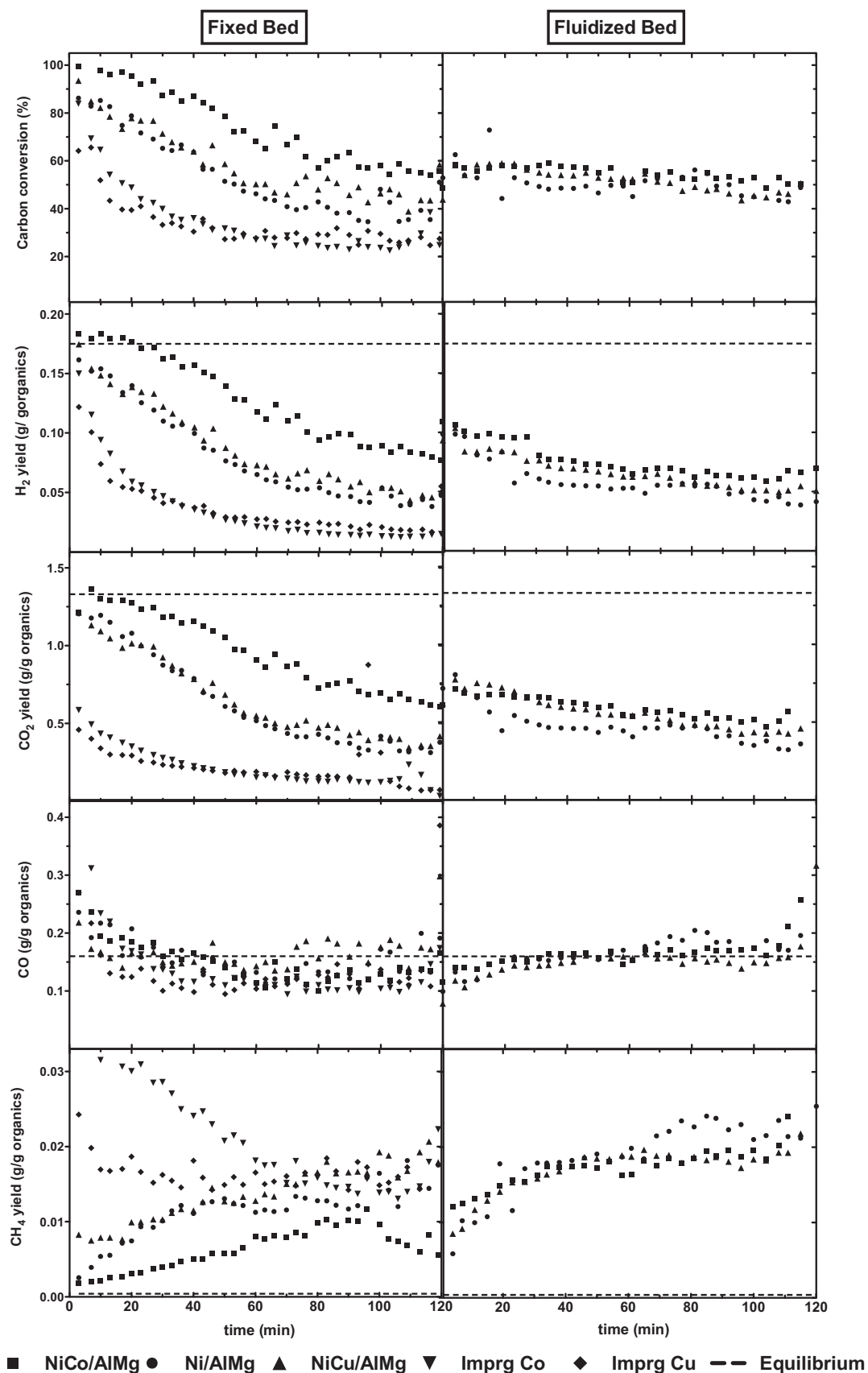


Fig. 5. Carbon conversion to gases (%), H₂, CO₂, CO and CH₄ yields (g/g organics) evolution with time for the Ni/AlMg, NiCo/AlMg, NiCu/AlMg, Imprg. Cu and Imprg. Co catalysts in fixed bed (left) and fluidized bed (right).

Table 4
Overall 2 h results (mean \pm standard deviation) of the catalysts in fixed bed and thermodynamic equilibrium. Experimental conditions: $t = 2$ h, $T = 650^\circ\text{C}$, $P = 1$ atm, $Q = 0.12$ mL/min, $W/m_{\text{org}} = 4$ g cat. min/g org., $G_{\text{C1 HSV}} = 13,000$ h $^{-1}$.

| | Carbon conversion (%) | H ₂ yield (g/g organics) | CO ₂ yield (g/g organics) | CO yield (g/g organics) | CH ₄ yield (g/g organics) |
|-------------|-----------------------|-------------------------------------|--------------------------------------|-------------------------|--------------------------------------|
| NiCo/AlMg | 80.0 \pm 4.5 | 0.138 \pm 0.006 | 1.014 \pm 0.066 | 0.181 \pm 0.011 | 0.007 \pm 0.002 |
| Ni/AlMg | 57.4 \pm 5.6 | 0.082 \pm 0.009 | 0.561 \pm 0.056 | 0.154 \pm 0.027 | 0.011 \pm 0.002 |
| NiCu/AlMg | 63.1 \pm 0.4 | 0.093 \pm 0.002 | 0.693 \pm 0.036 | 0.181 \pm 0.008 | 0.015 \pm 0.002 |
| Imprg. Cu | 50.0 \pm 1.7 | 0.050 \pm 0.001 | 0.375 \pm 0.016 | 0.194 \pm 0.001 | 0.029 \pm 0.003 |
| Imprg. Co | 43.0 | 0.042 | 0.310 | 0.167 | 0.025 |
| Equilibrium | 100 | 0.164 | 1.326 | 0.156 | 0.000 |

quick catalyst deactivation suffered by the impregnated catalysts. These impregnated catalysts might have suffered from sintering due to the fact that they were calcined for 6 h (3 h when preparing the reference catalyst used as support plus another 3 h after the impregnation of the active phase modifier) while the coprecipitated catalysts were calcined for 3 h. An increase in the calcination times favours the sintering of the catalysts [28,29].

As regards the type of modifier, it was observed that in the case of the coprecipitated catalysts the incorporation of Co (NiCo/AlMg catalyst) provided a better performance in terms of higher carbon conversion to gases and higher H₂ and CO₂ yields than the incorporation of Cu (NiCu/AlMg catalyst). No statistically significant differences in catalyst performance were found between this latter and the reference (Ni/AlMg) catalyst. This suggests that the addition of the studied amount of Cu as a modifier had no effect on the catalytic activity of the catalyst under the operating conditions tested. However, when the catalysts were modified by impregnation (Imprg. Co and Imprg. Cu), the effect of the type of modifier was not observed under the experimental conditions tested, which may indicate that the deactivation of the prepared catalysts is more dependent on the preparation method than on the metal used to modify them (Cu or Co).

The differences between the catalysts tested could be caused by the fact that the incorporation of Co by coprecipitation allows a higher extension of the reforming reaction as well as the subsequent water gas shift (WGS) reaction due to lower catalyst deactivation by coke. Thus, the incorporation of Co to the catalyst could facilitate the gasification of the coke deposited on the catalyst surface, could lead to the formation of a less deactivating coke and/or could reduce its formation rate. Fig. 5 shows the evolution of all these variables with time, where the trends fit with the ANOVA analysis results. The same homogeneous groups as those discussed above are identified. All the catalysts showed a loss of activity over time due to their progressive deactivation. It can be seen how the initial catalytic activity for all the coprecipitated catalysts was approximately the same, achieving almost complete initial carbon conversion to gases, and H₂ and CO₂ initial yields close to thermodynamic equilibrium. In contrast, the initial activity of the impregnated catalysts was lower. They both suffered quicker deactivation.

No statistically significant differences were found between the different catalysts tested in terms of the CO yield (p -value = 0.2704) because of the intermediate nature of the CO reaction. The CO

appeared as a product in the reforming reaction and subsequently disappeared in the water gas shift (WGS) reaction.

The ANOVA analysis of the CH₄ yield (p -value = 0.0021) indicates that at least one of the tested catalysts provided a statistically different yield from the others. Analysing the multiple range test (Table 5), three different homogeneous groups are detected. The highest CH₄ yield was obtained when using the two impregnated catalysts (Imprg. Co and Imprg. Cu). No statistically significant differences were found between them. High CH₄ yields were achieved from the beginning of the reforming reaction. This seems to confirm the higher initial deactivation of these impregnated catalysts, since CH₄ is not a product of the steam reforming reaction. The catalysts may have suffered deactivation by sintering, probably caused by their double calcination. However, when the catalysts were prepared by coprecipitation, the yield was influenced, though not very significantly, by the type of modifier used. The coprecipitated NiCo/AlMg catalyst provided the lowest CH₄ yield followed by the Ni/AlMg and NiCu/AlMg catalysts. In the case of these coprecipitated catalysts, the CH₄ yield was very close to the thermodynamic value at the beginning of the reaction, progressively increasing with time due to the catalyst deactivation. These results are in agreement with results of other authors [2,30] who related the catalyst deactivation with an increase in the CH₄ yield.

3.4. Results in the fluidized bed reactor

The overall 2 h results obtained in the steam reforming fluidized bed experiments using the Ni/AlMg, NiCo/AlMg, NiCu/AlMg coprecipitated catalysts as well as their corresponding thermodynamic equilibrium values are summarized in Table 6. The impregnated catalysts were not tested in the fluidized bed reactor due to their weak performance in the fixed bed. The statistical analysis of the results by means of an ANOVA analysis is presented in Table 7, where the p -values and the LSD homogeneous groups of catalyst for each response variable are given.

Fig. 5 shows the evolution over time of the carbon conversion to gas and the different gas yields in the fluidized bed. A small decrease can be observed for the carbon conversion to gases and the H₂ and CO₂ yields. This may indicate that the catalysts suffered from weak deactivation when used in the fluidized bed reactor. In addition, the initial carbon conversion to gases was not complete and the initial H₂ and CO₂ yields were far from the thermodynamic equilibrium value.

Table 5
ANOVA analysis and LSD homogeneous groups for carbon conversion and H₂, CO₂, CO, and CH₄ yields of the five catalysts tested in fixed bed.

| | Carbon conversion (%) | H ₂ yield (g/g organics) | CO ₂ yield (g/g organics) | CO yield (g/g organics) | CH ₄ yield (g/g organics) |
|---|-----------------------|-------------------------------------|--------------------------------------|-------------------------|--------------------------------------|
| p -Value | 0.0047 | 0.0004 | 0.0008 | 0.2704 | 0.0021 |
| Homogeneous groups (LSD test. 95% confidence level) | | | | | |
| NiCo/AlMg | A | A | A | A | A |
| Ni/AlMg | B | B | B | A | B |
| NiCu/AlMg | B | B | B | A | B |
| Imprg. Cu | C | C | C | A | C |
| Imprg. Co | C | C | C | A | C |

A, B and C represent homogeneous LSD groups for every response variable.

Table 6

Overall 2 h results (mean \pm standard deviation) of the catalysts in fluidized bed and thermodynamic equilibrium. Experimental conditions: $t = 2$ h, $T = 650^\circ\text{C}$, $P = 1$ atm, $Q = 0.76$ mL/min, $W/m_{\text{org}} = 4$ g cat. min/g org., $G_{\text{C1HSV}} = 13,000$ h $^{-1}$, $u/u_{\text{mf}} = 10$.

| | Carbon conversion (%) | H ₂ yield (g/g organics) | CO ₂ yield (g/g organics) | CO yield (g/g organics) | CH ₄ yield (g/g organics) |
|-------------|-----------------------|-------------------------------------|--------------------------------------|-------------------------|--------------------------------------|
| NiCo/AlMg | 56.2 \pm 0.8 | 0.084 \pm 0.004 | 0.638 \pm 0.121 | 0.152 \pm 0.034 | 0.015 \pm 0.005 |
| Ni/AlMg | 50.4 | 0.058 | 0.467 | 0.171 | 0.019 |
| NiCu/AlMg | 52.4 \pm 0.3 | 0.071 \pm 0.002 | 0.592 \pm 0.028 | 0.141 \pm 0.024 | 0.015 \pm 0.002 |
| Equilibrium | 100 | 0.164 | 1.326 | 0.156 | 0.000 |

The overall 2 h results and the ANOVA analysis reveal smaller differences between the catalysts in the fluidized bed compared to the fixed bed. The p -values obtained in the fixed bed for all the response variables are lower than their corresponding p -values obtained in the fluidized bed. This indicates that the differences between catalysts are higher in the fixed bed. The same homogeneous groups were detected in both types of bed for the overall carbon conversion to gases and the overall H₂ yield. The highest carbon conversion to gases (56.2 \pm 0.8%) and H₂ yield (0.084 \pm 0.004 g H₂/g organics) were achieved with the coprecipitated NiCo/AlMg catalyst. No differences were detected between the Ni/AlMg and NiCu/AlMg catalysts, as in the fixed bed. These small differences between the catalysts might explain why no significant differences were found in the CO₂ yields obtained with the catalysts tested (p -value = 0.4363).

Non-statistically significant differences between the catalysts were found in both CO (due to its condition as a reaction intermediate) and CH₄ yields in the fluidized bed experiments. As can be seen in Fig. 5, a progressive increase in the CH₄ yield over time took place, indicating progressive deactivation of the catalysts.

3.5. Comparison between fixed bed and fluidized bed

Comparing the experimental results obtained in the fixed and fluidized beds, it was found that in both installations the catalyst with the best performance was the coprecipitated NiCo/AlMg, followed by the coprecipitated Ni/AlMg and NiCu/AlMg catalysts without significant differences between them. Nevertheless, the difference between the performance of the NiCo/AlMg catalyst and the other two is statistically dependent on the gas–solid contact regime, being higher in the fixed bed reactor. The catalysts in the fluidized bed reactor, although less active due to their lower initial carbon conversion to gases and H₂ and CO₂ yields, suffered from lower deactivation. Their values were very stable over time. This lower deactivation could be a consequence of the gas–solid contact taking place in the fluidized bed reactor reducing the amount of coke deposited on the catalysts, improving their stability. Furthermore, due to the small inner diameter of the reactor (25.4 mm), a slugging regime could occur, diminishing the effective amount of catalyst in contact with the feed. This would imply an increase in the real mass of the catalyst/organic mass flow (W/m_{org}) ratio, there being less organic product in contact with the catalyst. The low initial carbon conversion to gases as well as the low H₂ and CO₂ initial yields could therefore be a consequence of the fact that a substantial amount of the feed would not come into effective

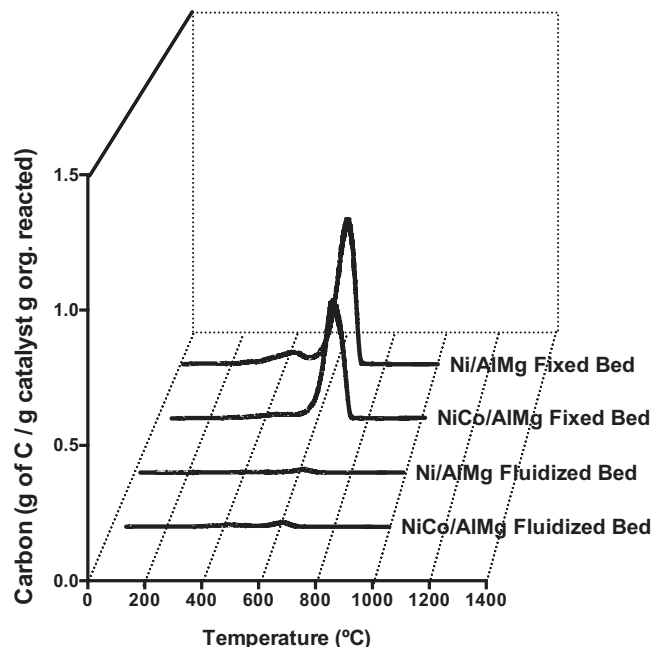


Fig. 6. TPO profiles for the Ni/AlMg and NiCo/AlMg catalysts used in fixed and fluidized bed.

contact with the catalyst, and consequently not deactivate it. This part of the feed would exit the fluidized bed reactor unreacted.

The higher carbon conversion and H₂ and CO₂ yields obtained at the beginning of the fixed bed experiments explain why the overall 2 h results were higher in the fixed bed reactor, despite the fact that the catalyst deactivation was higher in the fixed bed than in the fluidized bed.

The very demanding experimental conditions for the catalysts in the fixed bed led to the difference between the performance of the NiCo/AlMg catalyst and the other two being higher than in the fluidized bed, due to the greater stability of this catalyst compared to the others under tough experimental conditions. In contrast, in the fluidized bed, as explained above, the reforming condition could be less severe for the catalysts. This results in smaller differences between the catalysts tested, masking the catalyst effect.

No statistically significant differences were found between the overall CH₄ yields obtained in the two installations. Nevertheless, at the beginning of the fixed bed experiments the CH₄ yield was close to zero, which indicates good catalyst performance. In the

Table 7

ANOVA analysis and LSD homogeneous groups for carbon conversion and H₂, CO₂, CO, and CH₄ yields for the three catalysts tested in fluidized bed.

| | Carbon conversion (%) | H ₂ yield (g/g organics) | CO ₂ yield (g/g organics) | CO yield (g/g organics) | CH ₄ yield (g/g organics) |
|---|-----------------------|-------------------------------------|--------------------------------------|-------------------------|--------------------------------------|
| p -Value | 0.0266 | 0.0292 | 0.4363 | 0.7309 | 0.7428 |
| Homogeneous groups (LSD test. 95% confidence level) | | | | | |
| NiCo/AlMg | A | A | A | A | A |
| Ni/AlMg | B | B | A | A | A |
| NiCu/AlMg | B | B | A | A | A |

A and B represent homogeneous LSD groups for every response variable.

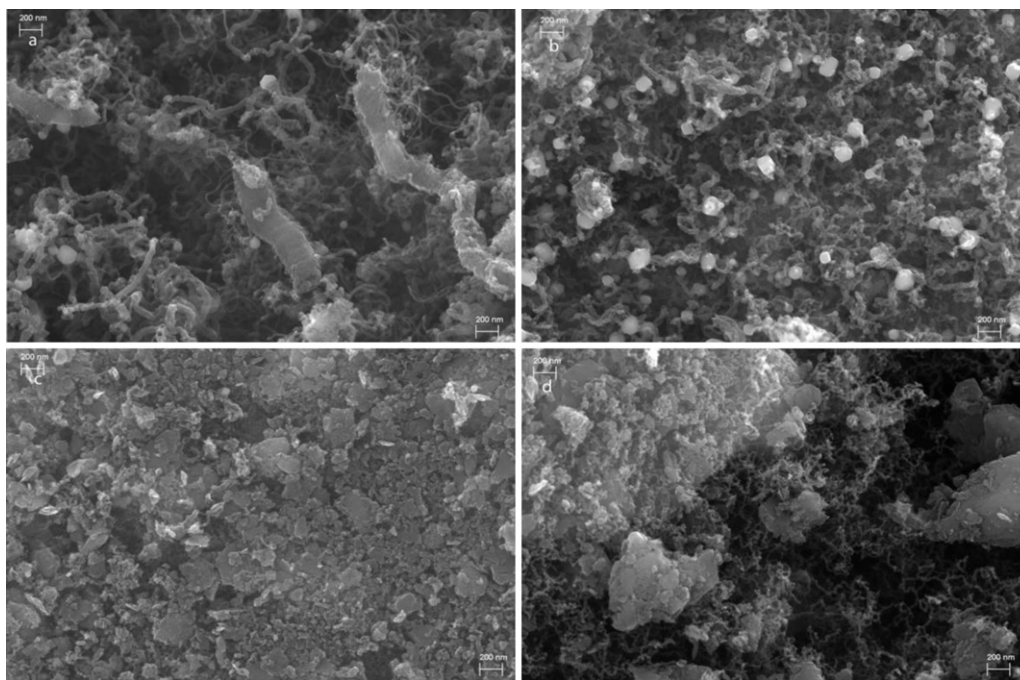


Fig. 7. FESEM images for the Ni/AlMg and NiCo/AlMg catalysts used in the fixed bed (a and b) and fluidized bed (c and d) reactors.

fluidized bed reactor, however, this value was far from zero, which suggests that a poor gas–solid contact took place.

3.6. Characterization of the catalysts after the reforming reactions

The loss of activity with time observed in the steam reforming experiments is mainly due to the deposition of coke on the catalyst surfaces. Elemental, temperature programmed oxidation (TPO) and field emission scanning electron microscopy (FESEM) analyses were carried out to quantify and characterize these carbon deposits. The analyses were only done on the Ni/AlMg and NiCo/AlMg catalysts used in the fixed and fluidized bed reactors to determine whether the most significant differences observed in terms of catalyst behaviour could be related to the kind and amount of coke deposited on the catalysts. Figs. 6 and 7 show the TPO profiles and FESEM images, respectively. The quantitative amount of coke has been calculated as g of C/g of catalyst g of organics reacted. This calculation has already been employed by Di Felice et al. [31] and makes the comparison between coke deposits more reliable. The characterization results for elemental and TPO analyses as well as the temperature of the TPO peaks and their corresponding amount of coke are listed in Table 8.

The total carbon content of the samples and the carbon content corresponding to each of the two peaks detected in the TPO analyses (mg C/g catalyst g organics) have been compared for each catalyst and each reactor making use of an analysis of variance (ANOVA) with 95% confidence. When the ANOVA analysis detected significant differences, the multiple range least significant difference (LSD) test with a significance level of 0.05 was employed. As a result of this analysis, the multiple range table was obtained. In this table the catalysts are classified in homogeneous groups using as many letters as different groups obtained. The results of this analysis for the total carbon content and each peak of the TPO analysis are provided in brackets in Table 8.

Fig. 6 shows the different kinds of coke deposits on the catalyst surfaces. Two different kinds of coke deposits are observed at temperatures of around 400 °C and 600 °C in the TPO analysis. The first peak may correspond to easily gasified coke. Martín et al.

[32] assigned the peak at 400 °C to the coke formed in the metal–support interface which contains CH_x species and/or surface carbon [33,34]. The peak at 600 °C consists of filamentous carbon, which is less deactivating but more difficult to oxidize. Goula et al. [35] assigned the high temperature peak to filamentous carbon. Similar results were reported by Medrano et al. [2].

The analysis presented in Table 8 shows a good concordance between the amounts of carbon calculated by elemental and TPO analyses. No statistically significant differences were found between the total amount of carbon deposits determined by the two techniques, with 95% confidence (p -value = 0.68). Comparing the quantity of coke deposited on the two catalysts used in the fixed bed and the fluidized bed reactor (Table 8), it can be appreciated how the total amount of carbon deposited on the catalysts statistically depends on the catalyst and the reactor used in the steam reforming experiments (p -value = 0.0001). Making use of the multiple range test, shown in Table 8, it can be concluded that for the two catalysts tested, the total amount of carbon deposited on the catalyst surfaces was higher when the steam reforming took place in the fixed bed reactor. This fact could justify why the catalyst deactivation observed for this system was higher than the deactivation observed for the fluidized bed reactor. In addition, in the fixed bed, the amount of carbon deposited on the Ni/AlMg catalyst was higher than the amount of carbon deposited on the NiCo/AlMg catalyst. This fact might explain the higher stability of the cobalt-modified catalyst. In contrast, in the fluidized bed reactor the total amount of carbon deposited on the two catalysts was not statistically different with 95% confidence.

Two peaks are detected in the TPO analysis (Fig. 6 and Table 8). The first peak is very low for the two catalysts in both installations, indicating a small formation of this type of coke. No statistically significant differences (p -value = 0.53) were found between the amount of carbon corresponding to this low temperature peak for the two catalysts tested in both installations. In contrast, the second peak is quite high in some samples indicating a substantial presence of this type of coke. In this case, statistically significant differences (p -value = 0.005) were found between the quantity of coke deposited in the four catalysts used (two in each reactor). The

Table 8

Carbon quantification results by elemental and TPO analyses for the Ni/AlMg and NiCo/AlMg catalysts used in fixed and fluidized bed expressed as mean \pm standard error (mg C/g catalyst g of organic reacted).

| Catalyst | Elemental analysis | TPO analysis | | | | |
|-------------------------|------------------------------------|------------------------------------|------------------------------|------------------------------------|------------------------------|------------------------------------|
| | Total carbon (mg C/g cat g org) | Total carbon (mg C/g cat g org) | T (1st peak) ($^{\circ}$ C) | C (1st peak) (mg C/g cat g org) | T (2nd peak) ($^{\circ}$ C) | C (2nd peak) (mg C/g cat g org) |
| Ni/AlMg fixed bed | 154 \pm 3 (A) | 165 \pm 3 (A) | 413 | 20 \pm 3 (A) | 610 | 143 \pm 1 (A) |
| NiCo/AlMg fixed bed | 120 \pm 3 (B) | 129 \pm 3 (B) | 413 | 8 \pm 3 (A) | 603 | 119 \pm 1 (B) |
| Ni/AlMg fluidized bed | 5 \pm 4 (C) | 4 \pm 3 (C) | 416 | 1 \pm 3 (A) | 604 | 3 \pm 1 (C) |
| NiCo/AlMg fluidized bed | 10 \pm 3 (C) | 10 \pm 2 (C) | 400 | 5 \pm 2 (A) | 580 | 4 \pm 1 (C) |
| p-Value | 0.0001 | 0.0001 | | 0.23 | | 0.005 |

Error has been calculated using a pooled estimate of error variance.

A, B and C represent statistically homogeneous LSD groups with 95% confidence.

ANOVA analysis of the total carbon content has been calculated employing both elemental and TPO results.

same homogeneous groups were obtained as for the total amount of carbon.

Analysing the FESEM images (Fig. 7), deposits of filamentous carbon can be clearly observed for all the catalysts tested in both reactors. These deposits are longer and thicker for the catalyst that was used in the fixed bed reactor than for the same catalysts used in the fluidized bed. As predicted by the TPO results, when the fixed bed reactor was used, longer, thicker and more abundant carbon filaments were formed on the Ni/AlMg catalyst than on the NiCo/AlMg catalyst.

The difference between the morphology and the structure of the carbon deposits observed in the catalysts when used in one reactor or the other may be due to many factors. In this study, it may be due to the reaction atmosphere. In the fixed bed reactor, the atmosphere may be different along the axis of the catalyst bed because of the conversion of the reaction gas. However, in the fluidized bed reactor the atmosphere is well back-mixed. In addition, the less effective gas–solid contact taking place in the fluidized bed reactor as well as the possible slugging regime originated during the experiments might explain why the amount of reactants having effective contact with the catalyst was lower. This also implies a lower amount of coke being deposited on the catalysts. It can also explain why the positive effect of cobalt was higher in the fixed bed reactor where the reforming conditions were more demanding for the catalysts. In contrast, the reforming conditions were less severe for the catalyst in the fluidized bed, masking the positive effect of the cobalt.

Fig. 8 presents a pictorial scheme of the reduced Ni/AlMg and NiCo/AlMg catalysts considering all the information obtained from the steam reforming experiments as well as the characterization of the carbon deposits.

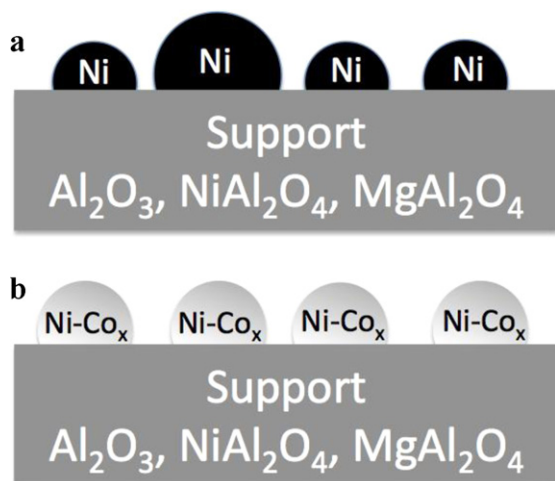


Fig. 8. Pictorial schemes of the reduced (a) Ni/AlMg and (b) NiCo/AlMg catalysts.

For the Ni/AlMg catalyst, two sizes of Ni crystallites are identified taking into account the size of the carbon filaments observed in the FESEM images. The bigger Ni crystallites could derive from the reduction of NiO species with low interaction with the support corresponding to the low temperature peak detected in the TPR analysis. These bigger crystallites may decrease the metal-support contact. This could have a significant influence on the steam reforming reaction and the gasification of the carbon intermediates [36,37].

For the NiCo/AlMg catalyst, considering both the TPR analyses and the FESEM images, small Ni crystallites with Co interaction are proposed. This catalyst could contain a higher amount of oxygen vacant sites and labile O on the support than the Ni/AlMg catalyst [36,37]. This might favour both the steam reforming reactions and the gasification of the carbon intermediates. Andonova et al. [27] explained that the addition of Co to the Ni/Al system significantly influences the metal-support interaction, which decreases the temperature of reduction of the catalysts.

According to the steam reforming results and the TPR analyses, an effective Ni–Cu interaction might not take place in the NiCu/AlMg catalyst.

In the case of the two catalysts prepared by impregnation, the supports might have a low amount of oxygen vacant sites and labile O that hinders the steam reforming reactions and favours the formation of carbon deposits [36,37]. In addition, because all the Cu content of the catalyst is reduced at low temperature according to the TPR results, it is proposed that the Ni–Cu interaction might not be significant for this catalyst. Neither may the interaction between Ni and Co for the Imprg Co catalyst be significant, according to the steam reforming results.

4. Conclusions

The catalytic steam reforming of an aqueous fraction (S/C = 7.6) of pine sawdust bio-oil has been studied in the present work using a fixed bed and a fluidized bed reactor. Five different research catalysts were prepared in the laboratory. A Ni/AlMg catalyst was selected as reference. Its modification with Cu or Co was studied, these promoters being incorporated by incipient wetness impregnation and by coprecipitation techniques. The main conclusions obtained from the present work are as follows:

1. Using the fixed bed reactor, the highest carbon conversion to gas as well as the highest H₂ and CO₂ yields were obtained when the coprecipitated cobalt modified catalyst (NiCo/AlMg) was used. The incorporation of the studied amount of Cu to the catalyst by coprecipitation did not provide statistically significant differences to the reference catalyst under the operating conditions tested. Both impregnated catalysts suffered from quick deactivation without significant

- differences between them. The catalyst performance was as follows: NiCo/AlMg > Ni/AlMg = NiCu/AlMg > Imprg. Cu = Imprg. Co.
- Identical tendencies in catalyst performance were found between the coprecipitated Ni/AlMg, NiCo/AlMg and NiCu/AlMg catalysts in the fluidized bed reactor, although the difference in terms of stability between them was lower than in the fixed bed.
 - The gas–solid contact had a significant influence on the catalytic steam reforming in general and on the catalyst deactivation in particular under the operating conditions tested. Using the fixed bed reactor, high initial carbon conversion to gas and high initial yields of H₂ and CO₂ close to their thermodynamic equilibrium values were achieved. Nevertheless, the catalysts suffered progressive deactivation over time. On the other hand, lower initial carbon conversion to gas as well as lower initial H₂ and CO₂ yields were obtained when the fluidized bed reactor was used, but the stability of the catalysts was higher. The gas–solid contact in the fluidized bed was less effective than in the fixed bed.
 - The characterization of the catalysts by elemental, TPO and FESEM analyses revealed a higher amount of coke deposited in the fixed bed reactor in comparison to the same catalysts used in the fluidized bed. This suggests that the gas–solid contact achieved in the fluidized bed reactor could decrease the effective amount of catalyst in contact with the feed, reducing its deactivation and consequently hindering thermodynamic H₂ and CO₂ yields under the operating conditions tested. Analysing the effect of the modifier, it was found that in the fixed bed reactor the introduction of Co into the catalyst by coprecipitation diminished the amount of coke deposits, allowing greater catalyst stability.

Acknowledgements

The authors wish to express their gratitude to the Aragón Government (project CTPP02/09) and the Spanish Ministerio de Ciencia e Innovación (MICINN) (project ENE-2010-18985) for providing financial support and the FPI grant awarded to Javier Remón Núñez (BES-2011-044856).

References

- [1] D. Ayhan, *Energy Conversion and Management* 49 (2008) 2106–2116.
- [2] J.A. Medrano, M. Oliva, J. Ruiz, L. García, J. Arauzo, *Energy* 36 (2011) 2215–2224.
- [3] X. Song, Z. Guo, *Energy Conversion and Management* 47 (2006) 560–569.
- [4] J.A. Medrano, M. Oliva, J. Ruiz, L. García, J. Arauzo, *International Journal of Hydrogen Energy* 33 (2008) 4387–4396.
- [5] L. García, R. French, S. Czernik, E. Chornet, *Applied Catalysis A: General* 201 (2000) 225–239.
- [6] R.M. Navarro, M.A. Pena, J.L.G. Fierro, *Chemical Reviews* 107 (2007) 3952–3991.
- [7] F. Bimbela, M. Oliva, J. Ruiz, L. García, J. Arauzo, *Journal of Analytical and Applied Pyrolysis* 79 (2007) 112–120.
- [8] F. Bimbela, M. Oliva, J. Ruiz, L. García, J. Arauzo, *Journal of Analytical and Applied Pyrolysis* 85 (2009) 204–213.
- [9] J.A. Medrano, M. Oliva, J. Ruiz, L. García, J. Arauzo, *Journal of Analytical and Applied Pyrolysis* 85 (2009) 214–225.
- [10] X. Hu, G. Lu, *Journal of Molecular Catalysis A: Chemical* 261 (2007) 43–48.
- [11] M.C. Ramos, A.I. Navascues, L. García, R. Bilbao, *Industrial & Engineering Chemistry Research* 46 (2007) 2399–2406.
- [12] S. Bona, P. Guillén, J.G. Alcalde, L. García, R. Bilbao, *Chemical Engineering Journal* 137 (2008) 587–597.
- [13] Y. Echegoyen, I. Suelves, M.J. Lázaro, M.L. Sanjuán, R. Moliner, *Applied Catalysis A: General* 333 (2007) 229–237.
- [14] N.M. Rodríguez, M.S. Kim, R.T.K. Baker, *Journal of Catalysis* 140 (1993) 16–29.
- [15] J. Chen, Y. Li, Z. Li, X. Zhang, *Applied Catalysis A: General* 269 (2004) 179–186.
- [16] F. Bimbela, D. Chen, J. Ruiz, L. García, J. Arauzo, *Applied Catalysis B: Environmental* 119–120 (2012) 1–12.
- [17] D. Wang, D. Montané, E. Chornet, *Applied Catalysis A: General* 143 (1996) 245–270.
- [18] D. Kunii, O. Levenspiel, *Fluidization Engineering*, second ed., Butterworth-Heinemann, Oxford, 1992.
- [19] K. Sipilä, E. Kuoppala, L. Fagernas, A. Oasmaa, *Biomass and Bioenergy* 14 (1998) 103–113.
- [20] A. Al-Ubaid, E.E. Wolf, *Applied Catalysis* 40 (1988) 73–85.
- [21] A. Monzón, N. Latorre, T. Ubieto, C. Royo, E. Romeo, J.I. Villacampa, L. Dussault, J.C. Dupin, C. Guimon, M. Montieux, *Catalysis Today* 116 (2006) 264–270.
- [22] A.J. Akande, R.O. Idem, A.K. Dalai, *Applied Catalysis A: General* 287 (2005) 159–175.
- [23] M. He, M. Luo, P. Fang, *Journal of Rare Earths* 24 (2006) 188–192.
- [24] A.M. Hilmen, D. Schanke, A. Holmen, *Catalysis Letters* 38 (1996) 143–147.
- [25] B. Jongsomjit, J. Panpranot, J.G. Goodwin Jr., *Journal of Catalysis* 204 (2001) 98–109.
- [26] A. Kogelbauer, J.G. Goodwin, R. Oukaci, *Journal of Catalysis* 160 (1996) 125–133.
- [27] S. Andonova, C.N. de Ávila, K. Arishtirova, J.M.C. Bueno, S. Damyanova, *Applied Catalysis B: Environmental* 105 (2011) 346–360.
- [28] D.N. Bangala, N. Abatzoglou, E. Chornet, *AIChE Journal* 44 (1998) 927–936.
- [29] L. García, M.L. Salvador, J. Arauzo, R. Bilbao, *Energy & Fuels* 13 (1999) 851–859.
- [30] S. Czernik, R. French, C. Feik, E. Chornet, *Fuel and Energy Abstracts* 44 (2003) 232.
- [31] L. Di Felice, C. Courson, P.U. Foscolo, A. Kiennemann, *International Journal of Hydrogen Energy* 36 (2011) 5296–5310.
- [32] N. Martín, M. Viniegra, R. Zarate, G. Espinosa, N. Batina, *Catalysis Today* 107–108 (2005) 719–725.
- [33] A. Djaidja, S. Libs, A. Kiennemann, A. Barama, *Catalysis Today* 113 (2006) 194–200.
- [34] J.d.S. Lisboa, D.C.R.M. Santos, F.B. Passos, F.B. Noronha, *Catalysis Today* 101 (2005) 15–21.
- [35] M.A. Goula, A.A. Lemonidou, A.M. Efstathiou, *Journal of Catalysis* 161 (1996) 626–640.
- [36] K. Polychronopoulou, C.N. Costa, A.M. Efstathiou, *Catalysis Today* 112 (2006) 89–93.
- [37] K. Polychronopoulou, A.M. Efstathiou, *Catalysis Today* 116 (2006) 341–347.